Available online at www.sciencedirect.com
SCIENCE DIRECT®
Journal of Organometallic Chemistry 683 (2003) 406–420
Journal of Organometallic Chemistry
www.elsevier.com/locate/jorganchem

# Preparation of models and oligomers of metal alkynyls NMR, GPC and X-ray structural characterization of building blocks for the construction of molecular devices

Alessandra La Groia [a], Antonella Ricci [a], Mauro Bassetti [a], Dante Masi [b], Claudio Bianchini [b], Claudio Lo Sterzo [c,*]

[a] *Istituto CNR di Metodologie Chimiche (IMC-CNR), Sezione Meccanismi di Reazione, Dipartimento di Chimica, Box 34-Roma 62, Università 'La Sapienza', Piazzale Aldo Moro 5, 00185 Rome, Italy*

[b] *Istituto CNR di Chimica dei Composti Organo Metallici (ICCOM), Area della Ricerca CNR, Via Madonna del Piano snc, 50019 Sesto Fiorentino (Firenze), Italy*

[c] *Dipartimento di Scienze degli Alimenti, Facoltà di Agraria, Università degli Studi di Teramo, Via Spagna 1, 64023 Mosciano S. Angelo (Teramo), Italy*

Received 2 June 2003

**Abstract**

A systematic study has been carried out for the use of the palladium-based Extended One Pot (EOP) synthetic protocol toward the preparation of metal alkynyl oligomers of general formula $[-C{\equiv}C-Ar-C{\equiv}C-M(L)_m-]_n$ (M = Pt, Pd). Model compounds of type *trans*-$M(PBu_3)_2(C{\equiv}CC_6H_5)_2$ have been prepared by the reaction of tributyltinethynylbenzene with *trans*-$M(PBu_3)_2Cl_2$, in the absence of palladium catalysis, since the presence of catalytic $Pd(PPh_3)_4$ yields reaction mixtures containing starting material, product and intermediate complex *trans*-$MCl(PBu_3)_2(C{\equiv}CC_6H_5)$. Palladium catalysis has been used for the formation of the bistinacetylide compounds $Bu_3Sn-C{\equiv}C-Ar-C{\equiv}C-SnBu_3$ (Ar = $C_6H_4$; bis(2,5-*n*-octyloxy)$C_6H_4$). Subsequent coupling of these compounds with $MCl_2(PBu_3)_2$ in the *absence* of palladium catalyst yields metal alkynyl oligomers. Comparison of $^{31}$P-NMR and gel permeation chromatography (GPC) analyses indicates that the GPC technique represents a reliable method to estimate polymer chain lengths for polymers bearing branched aromatic spacers, in spite of the rigid-rod shape of the polymer backbone. Single crystal X-ray determinations of model compounds demonstrate the essential role of side substituents in the aromatic ring to control the supramolecular order and, as a consequence, the optoelectronic properties of materials.


*Keywords:* Conjugated organometallic polymers; EOP synthesis; Palladium catalysis; Polymetallaaryleneethynylene

## 1. Introduction

The synthesis of conjugated organic and organometallic oligomers and polymers and the study of their properties have become a major focus in material science due to the interesting features of such materials for innovative optoelectronic applications [1]. Organometallic polymers incorporating transition metal centers bridged by conjugated polyynes (polymetallaacetylides) have actually a great potential as photonic or electronic wires. Indeed, the characteristic conjugation path of these materials allows the motion of either electronic excitation energy or electrons throughout the whole polymer chain, ultimately leading to conducting, magnetic and photoactive properties [2].

We have recently developed an innovative strategic route to poly(ethynylaromatic) polymers based on the preparation of aromatic tributyltinacetylide compounds and of their in-situ palladium-catalysed coupling with aromatic halides [3]. This new synthetic protocol, named Extended One Pot (EOP), essentially consists in a sequential *one-pot* multistep synthetic route which converts aromatic halides into aromatic acetylides, then into aromatic tributyltinacetylides and finally into

* Corresponding author.
*E-mail address:* losterzo@agr.unite.it (C. Lo Sterzo).

0022-328X/03/$ - see front matter © 2003 Elsevier B.V. All rights reserved.
doi:10.1016/j.jorganchem.2003.08.007

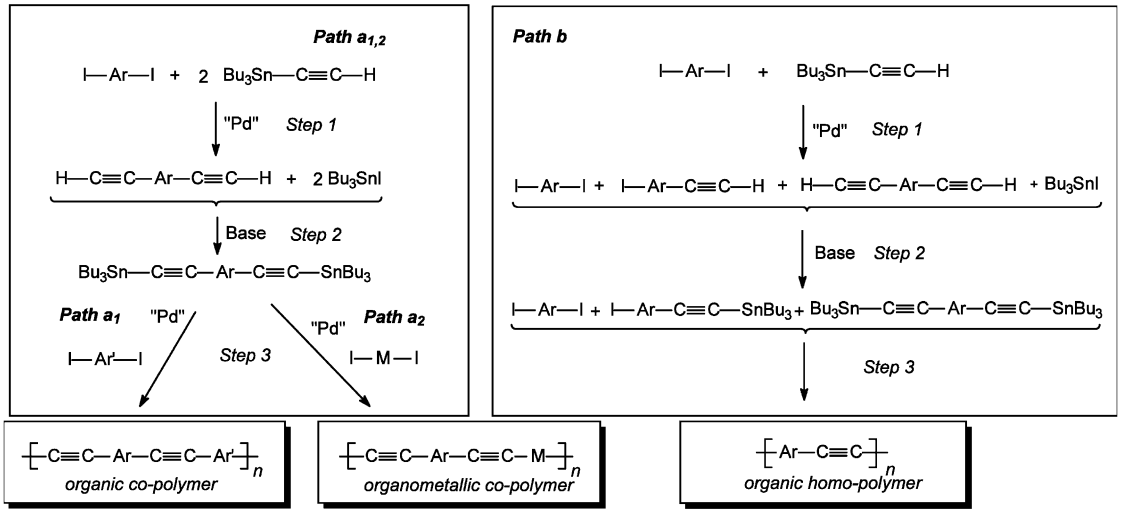


Fig. 1. Different uses of the EOP procedure.

poly(ethynylaromatic) polymers, the first and the third steps being palladium catalyzed. Depending on the nature of the coupling partners, the EOP synthetic protocol may be oriented towards the formation of either ethynylaromatic homo-polymers $[-C{\equiv}C-Ar-]_n$ (Fig. 1, Path b), or ethynylaromatic co-polymers $[-C{\equiv}C-Ar-C{\equiv}C-Ar'-]_n$ (Path $a_1$) [4]. The polymeric materials obtained by EOP method are characterized by comparable opto-electronic properties with those exhibited by similar materials prepared with conventional procedures [3b]. Therefore, the EOP synthetic protocol represents a simplified, well established and reliable synthetic procedure for the synthesis of an important class of materials.

Since metallaacetylide moieties can be prepared by coupling of metal-halides and trialkyltinacetylides by palladium catalysis [5], we have focussed our attention on the possibility of extending the EOP method to the preparation of ethynylaromatic–ethynylmetallo co-polymers $[-C{\equiv}C-Ar-C{\equiv}C-M(L)_m-]_n$, as indicated in path $a_2$ of Fig. 1. Although the formation of a large variety of model metallaacetylide compounds as well as of sophisticated organometallic tethers has been possible [6], insofar the synthesis of polymeric ethynylated organometallic materials by metal–carbon coupling under EOP conditions has been limited to the formation of short oligomers [3a,7]. Some adverse factors have been limiting the coupling to very few catalytic turnovers.

In view of the great potential represented by organometallic polymers as advanced materials for innovative applications [1,2], and of the appealing opportunities offered by the EOP method, we decided to perform a systematic study of the reactivity between metal halides (M = Pd, Pt) and trialkyltinacetylides, and then to optimize the conditions for the preparation of poly(aryleneacetylene-co-metallaacetylene) polymers of type $[-Ar-C{\equiv}C-M(L)_m-C{\equiv}C-]_n$ (M = Pt, Pd).

## 2. Results and discussion

The synthetic route outlined in path $a_2$ (Fig. 1) combines the straightforward *one-pot* Pd-catalyzed preparation of aromatic bistributyltinacetylides (steps 1 and 2) with a transmetalation reaction between metal halides and the tinacetylide groups, i.e. a metal–carbon bond-formation process (step 3). The successful combination of these synthetic sequences would provide a novel and convenient protocol for the synthesis of innovative materials with a diverse range of technological applications.

We envisaged that the encountered difficulties in obtaining high molecular weight materials in the preparation of organometallic polymers were due to lack of extended coupling, in particular that the conditions which led to the aromatic bistributyltinacetylide compounds (steps 1 and 2) were not suitable to perform with comparable efficiency the reaction between M–Cl and $Bu_3Sn-C{\equiv}C-$ functionalities. These unfavourable circumstances are probably the results of the complex factors governing the transmetalation process [8]. As a very preliminary approach we then decided to study the formation of model compounds of type *trans*-$M(PBu_3)_2(C{\equiv}CC_6H_5)_2$ (M = Pd, **4**; Pt, **5**), according to Scheme 1, by the reaction of tributyltinethynylbenzene (**1**) with *trans*-bis(tributylphosphine)palladiumdichloride, *trans*-$Pd(PBu_3)_2Cl_2$ (**2**), or with *trans*-bis(tributylphosphine)platinumdichloride, *trans*-$Pt(PBu_3)_2Cl_2$ (**3**), in the presence of a catalytic amount (5 mol%) of $Pd(PPh_3)_4$. The transformation depicted in Scheme 1 was designed as synthetic probe in order to find the very

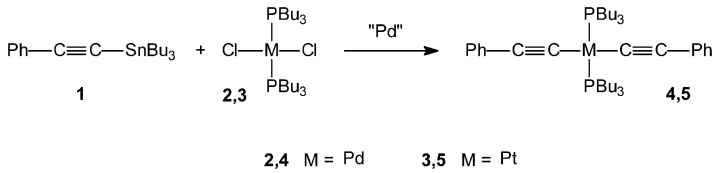


Scheme 1.

basic conditions to obtain efficiently metal acetylide moieties, and, in perspective, the most suitable conditions to perform step 3 in path $a_2$ (Fig. 1), under EOP conditions.

Formation of compounds **4**, **5** and of the intermediate monosubstituted *trans*-bis(tributylphosphine)(phenylacetylide)metalchloride complexes, *trans*-$MCl(PBu_3)_2(C{\equiv}CC_6H_5)$ (M = Pd, **6**; Pt, **7**) can be conveniently monitored by $^{31}$P-NMR spectroscopy. Trace a in Fig. 2 shows a typical spectroscopic pattern observed upon monitoring conversion of **3** into **7** and **5**, in the presence of the Pd catalyst. As a reference, the $^{31}$P-NMR spectra of authentic samples [9] of **3**, **5** and **7** are shown in traces b–d.

Since the EOP protocol leading to the ethynylated organic polymers had been previously observed to depend critically on both the temperature and the nature of the solvent [3b], the effect of these parameters on the reactions reported in Scheme 1 was preliminary analysed. In spite of the variety of conditions explored (different solvents, temperatures and reaction times), all the reaction mixtures contained, invariably and in comparable amount, the metaldichloride substrate together with both mono- and bis-ethynylated species. All

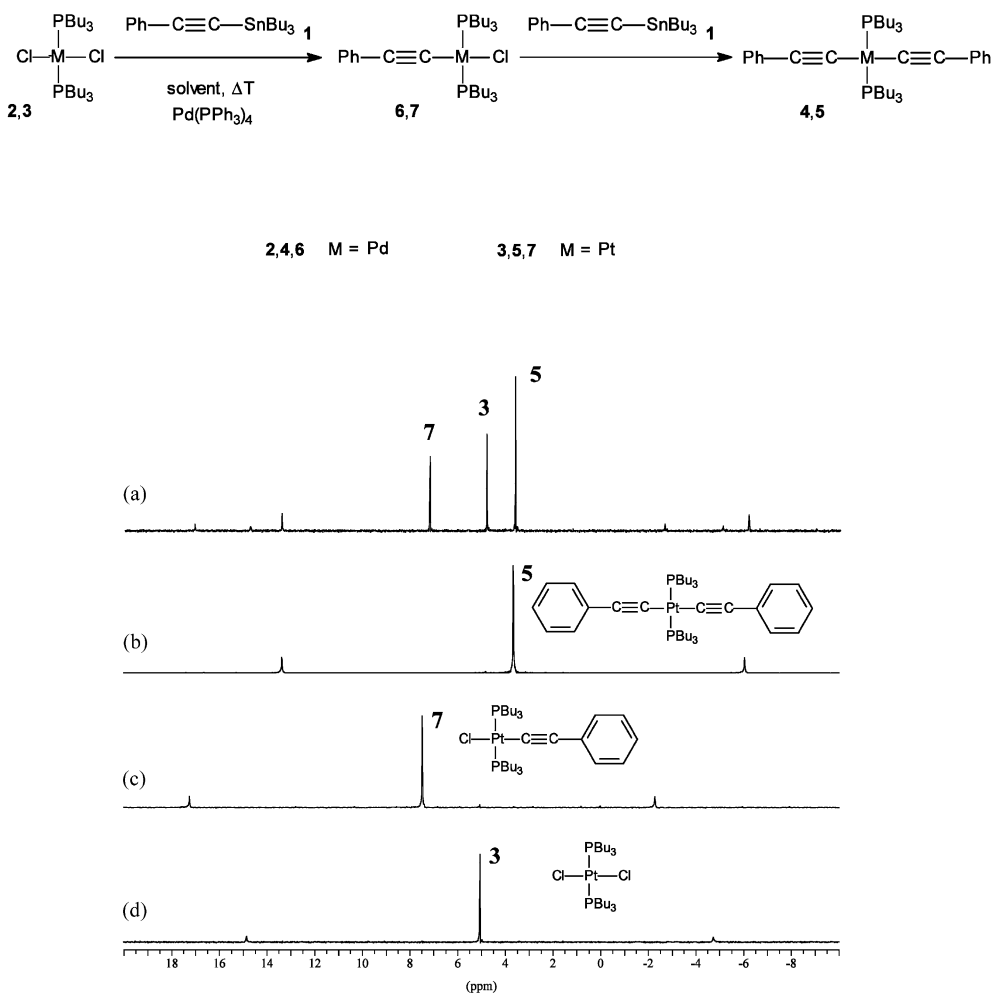


Fig. 2. (a) $^{31}$P-NMR spectrum of crude reaction mixture of **3** with **1**, carried out in THF at 70 °C for 20 h. (b–d) $^{31}$P-NMR of isolated **5**, **7** and **3**, respectively.

Table 1
Systematic study of reaction of **2** and **3** with **1**

| entry | | |  **2**[a] | 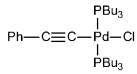 **6**[a] | 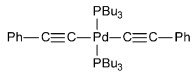 **4**[a] |
|---|---|---|---|---|---|
| 1 | THF | 25°C/20h | 79 | 9 | 12 |
| 2 | | 70°C/20h | 50 | 44 | 6 |
| 3 | DMF | 25°C/40h | 5 | 95 | |
| 4 | | 70°C/20h | **2** | **98** | |
| 5 | Dioxane | 25°C/40h | 12 | 26 | 62 |
| 6 | | 70°C/10h | | **5** | **95** |
| 7 | Toluene | 110°C/10h | | 58 | 42 |
| 8 | | 110°C/20h | | 47 | 53 |
| | | |  **3**[a] | 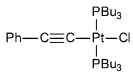 **7**[a] | 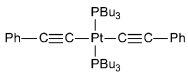 **5**[a] |
| 9 | THF | 25°C/20h | 100 | | |
| 10 | | 70°C/20h | 73 | 22 | 5 |
| 11 | DMF | 25°C/40h | 100 | | |
| 12 | | 70°C/40h | 51 | 17 | 32 |
| 13 | | 120°C/40h | 17 | 42 | 41 |
| 14 | Dioxane | 25°C/40h | 100 | | |
| 15 | | 110°C/40h | 13 | 62 | 25 |
| 16 | | 110°C/60h | | **89** | **11** |
| 17 | Toluene | 110°C/10h | 22 | 10 | 68 |
| 18 | | 110°C/20h | **3** | **5** | **92** |

[a]Reported amounts of compounds are obtained by $^{31}$P NMR and referred to an internal standard ($O{=}PPh_3$), 1:1 with respect to **2** or **3**).

our attempts to increase the low conversion of the starting material either by raising the temperature or prolonging the reaction time were unsuccessful, mixture of products being invariably obtained. Even the addition of a larger amount of Pd catalyst to the reaction mixture did not improve the yield; in some cases a reverse effect was observed, in fact [10]. Indeed, it has not been possible so far to achieve the selective formation of either mono- (**6**, **7**) or di-substituted (**4**, **5**) products. It is very likely that $Pd(PPh_3)_4$ catalyses the transformations of **2**–**3** into **6**–**7** and of **6**–**7** into **4**–**5** as well as the reverse processes. Therefore, higher temperatures, prolonged reaction times, and higher catalyst loadings would simply favour an equilibration process of the various compounds and produce reaction mixtures with compositions controlled by the relative thermodynamic stability of the various species involved. This hypothesis is in line with the formation of oligomers, rather than polymers, as occurred to us using the Pd-catalysed coupling of **2** or **3** with bis(trialkylethynyl)aromatic derivatives to prepare organometallic ethynylated polymers [3a,7]. The same limiting role of the EOP procedure has also been experienced by Fratoddi in the preparation of Pt and Pd poly-ynes [11].

The formation of ruthenium acetylides by coupling of tributyltinacetylides with ruthenium chlorides has been described by Wolf and co-workers [12], while Lewis and co-workers has shown that organometallic ethynylated materials, with a high degree of polymerisation, can be obtained by the reaction of trimethyltinacetylides with M–Cl moieties (M = Fe, Ru, Os, Rh, Co, Ni, Pd, Pt), with no need of Pd catalysis [13]. These reports as well as

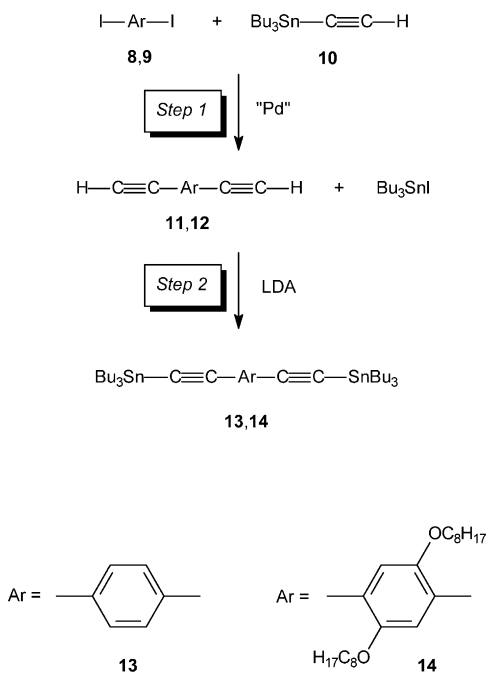


Scheme 2.

the lack of a clean transformation of **2** and **3** into **4** and **5**, respectively, indicate that the Pd catalyst may have an adverse role in the quantitative conversion of M–Cl and tributyltinacetylide moieties into metal acetylide species, for M = Pd or Pt.

Coupling reactions of **2** and **3** with **1** were then repeated in the absence of any Pd catalyst. As a result (Table 1), the selective formation of **6** (entry 4), **7** (entry 16), **4** (entry 6) and **5** (entry 18) was achieved. As compared to the Pd compounds **6** and **4**, more severe conditions, in terms of temperature and reaction time, were generally required for the formation of the corresponding Pt derivatives **7** and **5**.

Irrespective of the metal centre, the experimental conditions for the preparation of the mono-substituted complexes **6** and **7** (entries 4 and 16) were markedly different from those leading to the disubstituted complexes **4** and **5** (entries 6 and 18). Interestingly, the use of an excess of tributyl(phenylethynyl)tin in the synthesis of the mono-substituted complexes did not produce any disubstituted complex, which means that, irrespective of the stoichiometry, the formation of **6** and **7** is inherently favoured over that of **4** and **5**. The discovery of the appropriate conditions to obtain selectively either mono- or bis-phenylacetylides represents an appealing opportunity for the synthesis of different chemical modules to be used for engineering more elaborate aggregates.

Having established the most suitable protocol for the formation of the acetylide moieties M–C≡C–Ar (M = Pd, Pt), we focused our attention towards their potential use as building blocks for the preparation of the corresponding organometallic polymers $[-M-C{\equiv}C-Ar-C{\equiv}C-]_n$. To this purpose, an appropriate modification of the Pd-based EOP synthetic protocol was designed. The 1,4-bis(tributyltinethynyl)aryl derivatives **13** and **14** were obtained by a conventional EOP procedure. In the first step (Scheme 2), the Pd-catalysed coupling between the 1,4-diiodoaryl compounds **8** and **9** (aryl = $C_6H_4$, **8**; bis(2,5-*n*-octyloxy)$C_6H_4$, **9**) and tributyl(ethynyl)tin (**10**) gave the 1,4-diethynylaryl derivatives **11** and **12**, respectively, together with $Bu_3SnI$ as byproduct. In the following step, the deprotonation of the acetylide functionalities of **11** and **12** by LDA allowed the reaction with $Bu_3SnI$ to give **13** and **14**, respectively. At this stage, the Pd catalyst used in step 1, still present and active in the reaction medium, was removed to allow for the coupling of **13** and **14** with *trans*-$M(PBu_3)_2Cl_2$. Therefore, at the end of step 2 complexes **13** and **14** were isolated and purified from catalyst residues, and then allowed to react further.

With the aim of obtaining polymeric materials of type $[-M-C{\equiv}C-Ar-C{\equiv}C-]_n$, the reactions between *trans*-$Pt(PBu_3)_2Cl_2$ and the tin derivatives **13**, **14** were performed using the conditions which were found suitable for the formation of the di-substituted Pt compound **5**, namely in toluene at 110 °C (entry 18, Table 1), while *trans*-$Pd(PBu_3)_2Cl_2$ was reacted with **13**, **14** in dioxane at 70 °C, as for the preparation of the di-substituted Pd compound **4** (entry 6, Table 1). Polymeric materials **15**–**18** (Scheme 3) formed after prolonged heating (9–27 h), and were separated as brown residues after cooling at room temperature and partial removal of the reaction solvent. In the case of the coupling of *trans*-$M(PBu_3)_2Cl_2$ with the unbranched compound 1,4-bis(tributyltinethynyl)benzene (**13**) the solid products (Pd, **15**; Pt, **17**) appeared as yellow–brown crispy powders, while the alkyl-branched bis(tributyltin)ethynylaryl derivative **14** formed products **16** (Pd) and **18** (Pt) as brown gummy oils. Since both the mother liquors of the reactions and the methanol washings were still intensely coloured, the nature of the dissolved products was further analysed (vide infra).

The yellow powder obtained from the reaction of **3** with **13**, ($[-Pt(PBu_3)_2Pd-C{\equiv}C-C_6H_4-CC-]_n$), is soluble in dichloromethane, tetrahydrofuran and chloroform. The $^{31}$P-NMR spectrum of this material in $CDCl_3$ consists of two singlets at $\delta$ 7.4 ($J_{P-Pt}$ = 2366 Hz) and 3.5 ppm ($J_{P-Pt}$ = 2355 Hz) in a relative ratio of 1:1.3. On the basis of the close similarity between these values and those shown by **7** and **5**, the two signals were attributed to terminal $[-C{\equiv}C-Pt(PBu_3)_2Cl]$ and internal $[-C{\equiv}C-Pt(PBu_3)_2-C{\equiv}C-]$ phosphorus atoms, respectively. Noteworthy, the 1:1.3 relative ratio is consistent with the formation of the oligomeric mixture shown in Fig. 3.

The solution from which **17a** was separated and the rinsing methanol solution were collected and evaporated

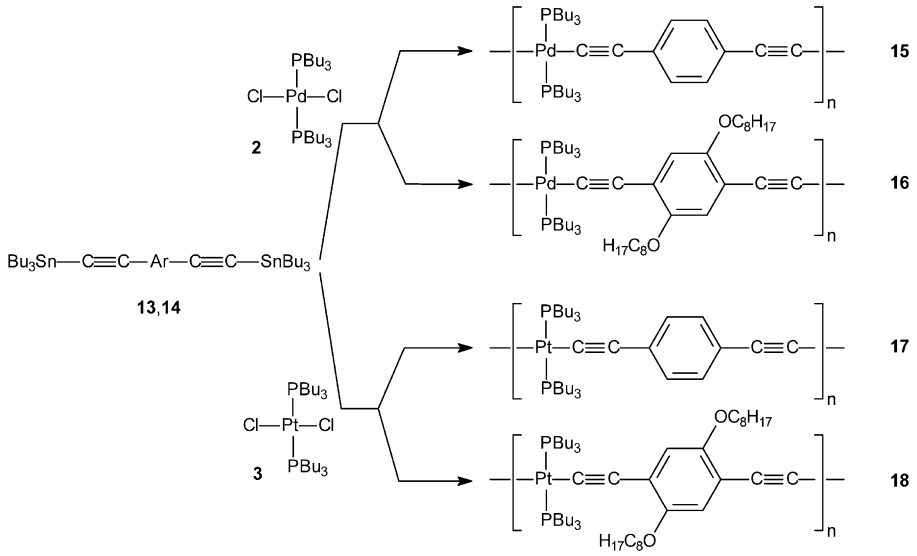


Scheme 3.

to give a brown oily residue. Chromatographic separation of this material afforded $Bu_3SnCl$ and a yellow solid, which was identified as the bimetallic compound **20** (ca. 20%), on the basis of its spectroscopic and analytical data (Fig. 4).

Similar results were obtained by reacting **3** with **14**. The gummy precipitate obtained upon addition of methanol to the concentrated reaction solution showed two signals in the $^{31}$P-NMR spectrum. The 1:1 intensity ratio and the chemical shifts ($\delta = 7.6$ ($J_{P-Pt} = 2368$ Hz) and 3.9 ($J_{P-Pt} = 2364$ Hz)) of these signals were unequivocally consistent with the formation of tetramer **18**. As described before, the solution recovered after separation of the precipitate and the methanol washings were evaporated to give a solid residue constituted by the bimetallic compound **22**, which was purified by chromatography.

The Pd complex **2** was reacted with either **13** or **14** under appropriate experimental conditions to give extended coupling with tributyltinacetylide functionalities (dioxane, 70 °C, see entry 6, Table 1). However, the material isolated contained low oligomers only. In the case of **15,** a $^{31}$P{$^1$H}-NMR analysis did not help to estimate the chain lengths, because the signals of the terminal and internal phosphorus atoms exhibited very close chemical shifts, and hence appeared as unresolved resonances. For this reason, the chain lengths were best estimated by gel permeation chromatography (GPC) (vide infra). The characterisation of the products dissolved in solution after precipitation of oligomers **15** and **16** was more rewarding. In both cases, the evaporation of the solvent, followed by chromatographic separation, gave **19** and **21** in pure form, which were recrystallised from dichlorometane–methanol to get single crystals suited for X-ray diffraction analyses (vide infra).

It is worth noting that, despite the use of a precise 1:1 stoichiometry, the reaction between **3** and **13** gave

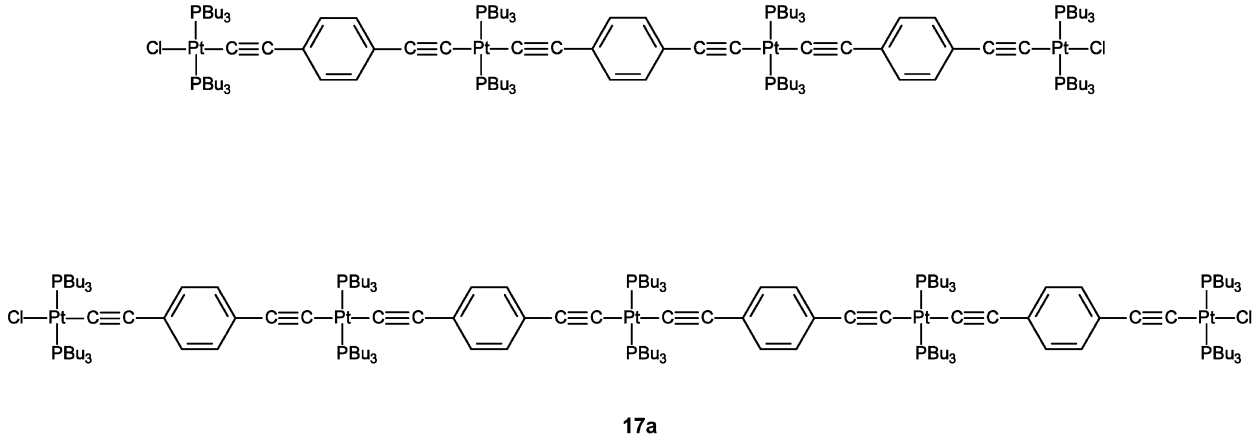


Fig. 3. Chains of different length of polymer **17a**.

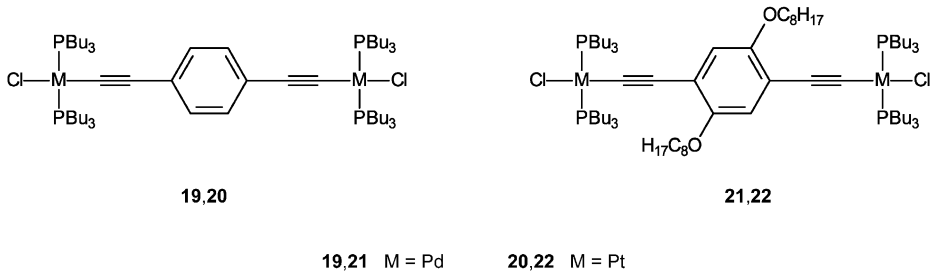


Fig. 4. Binuclear palladium and platinum complexes.

invariably the bismetallic-capped short-chain oligomers **20** and **17a**. A similar result was obtained by reacting **3** and **14** and **2** with either **13** or **14** (vide infra). These results may be explained in two ways: (i) under the experimental conditions adopted, the tinacetylides **13** and **14** are not as active as expected; (ii) these tinacetylides undergo appreciable degradation. The latter hypothesis is more likely as an increase in the concentration of **13** by 50% resulted in the formation of the dodecameric product **17b** [14]. Although the use of an excess of the bistinacetylide may represent a drawback, it should be considered that this coupling partner is conveniently accessible in large scale by the use of the EOP synthetic protocol. Therefore, in consideration of the importance of polymetallaacetylides in material science, the overall synthetic route remains of interest.

Evidence for the presence of longer chain lengths in **17b** was provided by UV absorption measurements. Fig. 5 shows the UV spectra of oligomers **17a** ($n = 4 \div 5$) and **17b** ($n = 12$), together with those of the corresponding block precursors **3** and **13**, and of dimer **20**. The $\lambda_{max}$ values in the spectra of **17a** and **b** were appreciably shifted as compared to the binuclear complex **20**, and remarkably shifted as compared to the $\lambda_{max}$ values of the starting monomers **3** and **13**. Interestingly, the 10 nm red shift between **17a** and **b** well accounts for the observed chain elongation in the latter. It may be therefore concluded that oligomers **17a** and **b** exhibit increased electronic conjugation, hence they would be featured by more efficient electron mobility, as compared to the corresponding precursor.

### 2.1. X-ray structural analysis of complexes *19* and *21*

Single crystals of **19** and **21** suitable for X-ray diffraction analysis were grown by slow evaporation of

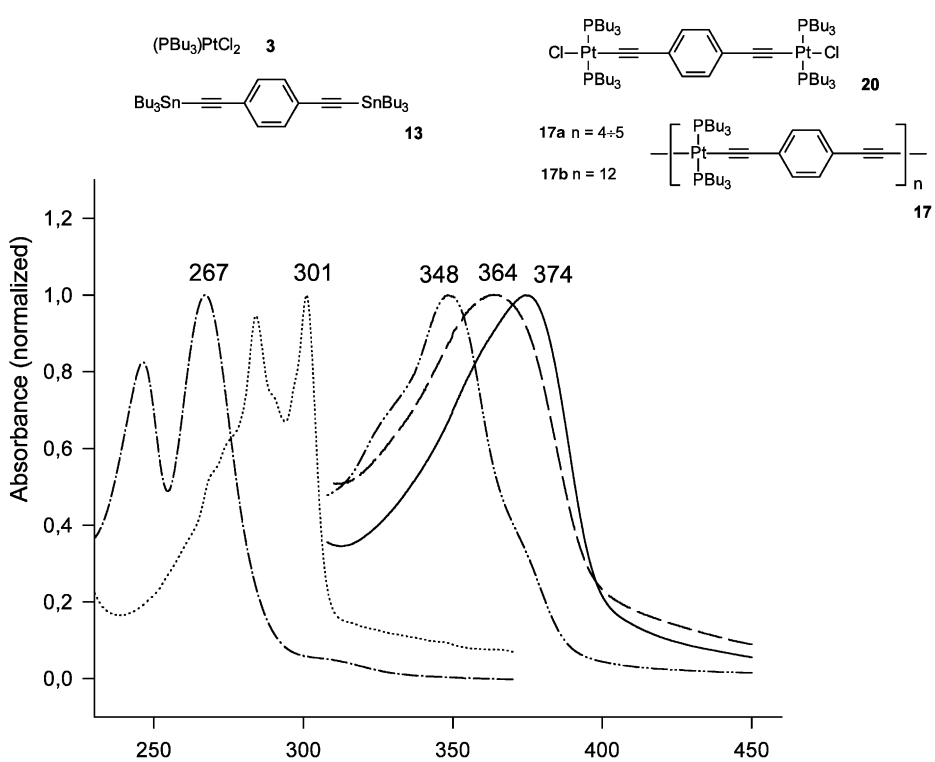


Fig. 5. UV–vis spectra in $CH_2Cl_2$.

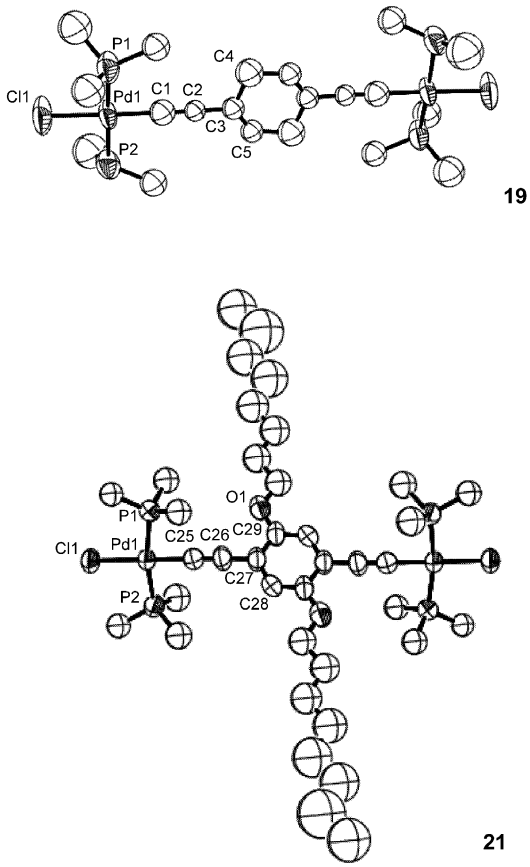


Fig. 6. ORTEP drawings of binuclear complexes **19** and **21**. Butyl groups have been omitted for clarity.

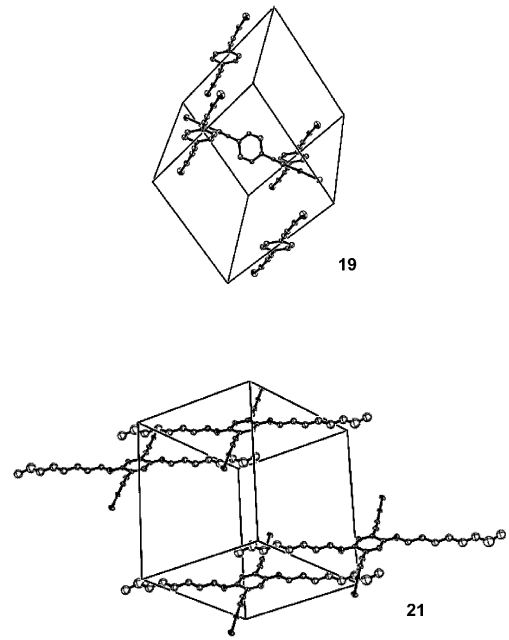


Fig. 7. ORTEP of complexes **19** and **21** showing the unit cell. The tributylphosphine groups have been omitted for clarity.

Table 2
Selected bond distances (Å) and angles (°) for **21**

| | |
|---|---|
| *Bond distances* | |
| Pd(1)–C(25) | 1.938(10) |
| Pd(1)–P(1) | 2.306(3) |
| Pd(1)–P(2) | 2.307(3) |
| Pd(1)–Cl(1) | 2.334(2) |
| C(25)–C(26) | 1.199(12) |
| C(26)–C(27) | 1.437(13) |
| C(27)–C(28) | 1.374(13) |
| C(27)–C(29) | 1.386(13) |
| O(1)–C(29) | 1.368(12) |
| *Bond angles* | |
| C(25)–Pd(1)–P(1) | 85.4(3) |
| C(25)–Pd(1)–P(2) | 84.8(3) |
| P(1)–Pd(1)–P(2) | 169.09(10) |
| C(25)–Pd(1)–Cl(1) | 178.9(3) |
| P(1)–Pd(1)–Cl(1) | 95.11(10) |
| P(2)–Pd(1)–Cl(1) | 95.56(10) |
| C(26)–C(25)–Pd(1) | 179.2(10) |
| C(25)–C(26)–C(27) | 174.1(12) |
| C(28)–C(27)–C(29) | 116.7(9) |
| C(28)–C(27)–C(26) | 121.7(9) |
| C(29)–C(27)–C(26) | 121.6(10) |

dichloromethane–methanol solutions at room temperature. The molecular structures of both complexes **19** and **21** are shown in Fig. 6. Selected bond distances and angles for **21** are listed in Table 2.

In either case, the crystal structure consists of a bimetallic capped 1,4-benzenediyl unit in which the two $Pd^{II}$ atoms are square-planarly coordinated by two trans tributylphosphines and by trans chlorine and acetylide moieties. The benzenediyl unit in **21** is decorated in positions 2,5 by octyloxy arms. Compound **21** contains half molecule in the asymmetric unit. In Fig. 6 is shown the complete molecule in which the butyl groups have been partially omitted for clarity. Because of the low quality of the experimental data, the butyl groups in the structure of **19** are not well defined. For this reason, only the structural data of **21** will be discussed and the rough data of **19** will be used just to confirm the connectivity in this compound.

In both compounds, the C≡C separations (1.199(12) Å in **21**, 1.19(4) Å and 1.18(4) Å in **19**) and the Pd–C separations (1.938(10) Å in **21**, 1.98(4) Å and 1.95(4) Å in **19**) are typical for metal-σ-acetylide moieties [15,16]. On the other hand, a partial conjugation within the molecule of **21** is put in evidence by the C≡C bond distances, which are longer than typical C≡C bonds and by the C26–C27 bonds which are shorter than typical C–C bonds.

The aromatic rings in **19** and **21** are essentially coplanar with the P–Pd–P axes, and the angle 179.2(10)° in **21** for the fragment Pd–C≡C confirms the linear geometry of the bis(acetylide) complexes [17].

The slight deformation of the square-planar geometry around the palladium centres (P(1)–Pd(1)–Cl(1) 95.11(10)° and P(2)–Pd(1)–Cl(1) 95.56(10)° in **21** [17] may be due to a repulsive interaction between the Cl and the phosphine ligands.

While the intrinsic structural features of **19** and **21** are comparable to those reported for several analogous compounds [15,16c,18], it is worth highlighting the mutual orientation of the different molecular units in the cell (Fig. 7, the H atoms and the $PBu_3$ groups have been omitted for clarity). Indeed, complex **19**, containing an unsubstituted phenyl ring as spacer between the acetylenic groups, shows two very different orientations of the molecules in the unit cell. In particular, a molecule is diagonally oriented with respect to the planes of two perfectly aligned molecules. The plane of the benzene ring of this diagonally-interposed molecule is almost perpendicular to the benzene planes of the surrounding molecules. In contrast, all the molecules composing the unit cell of **21** are well defined, perfectly layered along planes and aligned to each other.

The octyloxy side chains are laterally extended, with the two oxygen atoms and all the carbon atoms of the chains perfectly coplanar with the carbon atoms of the benzene ring. Within the same plane, the metal-chloride terminus of one molecule is oriented towards the midpoint of the octyloxy side chains of the preceding and following molecules. The octyloxy side chains are perfectly aligned between different horizontal planes and stacked in an interdigitated fashion. The aromatic rings between the planes are staggered, probably in consequence of the steric hindrance of the butyl groups.

The crystal structure of **21**, which represents a model molecule of an organometallic ethynylated polymer, sheds light on the key role of the side chains in controlling the orientation of the molecules. In parti-

Table 3
Yields and molecular weights for polymers and model complexes

| | | yield (%) | $M_W$[a] | $M_n$[b] | MWD[c] | DP($M_W$)[d] | DP($M_n$)[e] | DP(NMR)[f] | actual MW[g] | $M_n$/MW |
|---|---|---|---|---|---|---|---|---|---|---|
| polymer | | | | | | | | | | |
| **15**[h] | 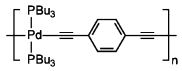 | 53 | 6940 | 3730 | 1.9 | 11 | 6 | | | |
| **16** | 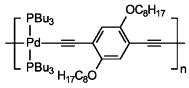 | 49 | 13480 | 7470 | 1.8 | 15 | 8 | 6 | | |
| **17a** | 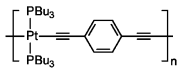 | 66 | 16020 | 8660 | 1.9 | 22 | 12 | 4÷5 | | |
| **17b** | | 70 | 48950 | 16380 | 3.0 | 68 | 23 | 12 | | |
| **18** | 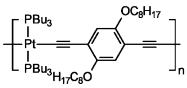 | 51 | 7020 | 3660 | 1.9 | 7 | 4 | 4 | | |
| model | | | | | | | | | | |
| **19** | 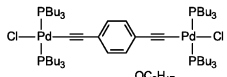 | | 3660 | 2810 | 1.3 | | | | 1217 | 2.3 |
| **21** | 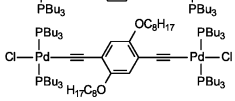 | | 2930 | 2380 | 1.2 | | | | 1474 | 1.6 |
| **20** | 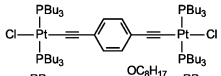 | | 3330 | 2590 | 1.3 | | | | 1394 | 1.9 |
| **22** | 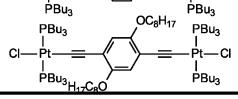 | | 4060 | 3050 | 1.3 | | | | 1651 | 1.8 |

[a]Weight average molecular weights. [b]Number average molecular weights. [c]Molecular weight distribution ($M_W/M_n$).
[d]Degree of Polymerization calculated on the basis of the $M_W$ value. [e]Degree of Polymerization calculated on the basis of the $M_n$ value.
[f] Degree of Polymerization calculated by $^{31}P$ NMR on the basis of terminal *vs* internal relative intensities of phosphorous signals.
[g]Molecular Weight. [h]unresolved $^{31}P$ NMR signal.

cular, the structure of **21** provides support to previous reports according to which rigid-rod polymers can form highly crystalline layered solids when functionalised with long aliphatic side chains [19], with influence on their (opto)electronic properties [20]. The supramolecular order of rigid-rod side-branched structures has been previously figured out by means of STM data [21] or deduced from X-ray powder diffraction data [22]. To the best of our knowledge, the structure of **21** is the first example of a single crystal X-ray determination showing the ordinate supramolecular assembling of long-chain decorated compounds.

### 2.2. Molecular weight determinations of products 15–22

The molecular weight of materials obtained from the coupling of 1,4-bis[(tributyltin)ethynyl]benzene (**13**) or 1,4-bis[(tributyltin)ethynyl]-2,5-di(octyloxy)benzene (**14**) with *trans*-$Pd(PBu_3)_2Cl_2$ (**2**) and *trans*-$Pt(PBu_3)_2Cl_2$ (**3**) were estimated by GPC, using polystyrene standards for the calibration, and by $^{31}$P-NMR spectroscopy. In Table 3 are reported the molecular weight, the molecular weight distribution and the degree of polymerisation of the different materials obtained; the Table also contains the degree of polymerisation as estimated by NMR integration of the terminal vs. internal relative intensities of the signals.

It is worth mentioning that the determination of the molecular weight of rigid-rod materials via GPC, is commonly considered unreliable. In fact, using randomly coiled polystyrene as calibration standard, the molecular weight of rigid-rod materials may be greatly overestimated [23]. For this reason, the determination of the chain length by integration of the NMR signals of the internal vs. external groups is considered as much more reliable. A comparison of the chain lengths obtained from either $^{31}$P-NMR or GPC analysis on **17a** and **b** showed the expected discrepancy. The GPC technique overestimated the molecular weights of **17a** and **b** because the rigid rod shape of these molecules magnify their hydrodynamic volume with respect to that of the polystyrene standard of analogous molecular weights. In contrast, the $^{31}$P-NMR and GPC ($M_n$) data for **18**, bearing two octyloxy substituents, were perfectly coincident, thus indicating that the two long side-substituents mask somehow the rigid rod structure of the polymer backbone and make the overall structure of **18** and **16** more similar to random coil polystyrene standards [23c]. The effect of the octyloxy arms is also evident by comparing the molecular weights of **21** and **22** obtained from $^{31}$P-NMR and GPC analyses ($M_n$/MW ratio in Table 3). In the case of **19** and **20**, containing an unsubstituted benzene ring, the discrepancy between $M_n$ determined by GPC and the actual MW is apparently higher as compared to the octyloxy-arm containing **21** and **22**.

## 3. Conclusions

The coupling of bistributyltinacetylides with M–Cl moieties (M = Pd, Pt) does not take place efficiently in the presence of $Pd(PPh_3)_4$, leading to an equilibration mixture of different products. In the absence of the Pd catalyst, however, the selective formation of short oligomers occurs, yet much harsher conditions are required. Since tinacetylides are easily accessible by the EOP protocol, the overall synthetic procedure shows a great potential for the preparation of metal acetylide polymers.

The combined use of $^{31}$P-NMR and GPC techniques has allowed to understand the limits as well as the reliability of both techniques in the estimation of polymer chain length for rigid rod-like materials. In particular we have offered a point of reconciliation to the widely debated opportunity of using GPC techniques in the molecular weight calculation for this class of materials.

The structural features of complexes **19** and **21**, studied by single crystal X-ray analysis, have demonstrated that with the proper choice of side substituents it is possible to control the supramolecular order, and in perspective, the electronic and optical properties of materials that are strongly influenced by solid-state arrangement.

## 4. Experimental

### 4.1. General procedures

Elemental analysis were performed by the Servizio Microanalisi of the Dipartimento di Chimica of Università di Roma 'La Sapienza'. IR spectra were recorded on a Nicolet FT 510 instrument in the solvent subtraction mode, using a 0.1 mm CsI cell or polyethylene disk. UV spectra were recorded on a Perkin–Elmer Lambda 18 spectrophotometer. $^1$H-, $^{13}$C- and $^{31}$P-NMR spectra were recorded on a Bruker AC300P spectrometer at 300, 75 and 121 MHz, respectively. Chemical shifts (ppm) are reported in $\delta$ values relative to $Me_4Si$; for $^1$H-NMR, $CHCl_3$ ($\delta$ 7.24) and for $^{13}$C-NMR, $CDCl_3$ ($\delta$ 77.0) were used as internal standard. The $^{31}$P-NMR chemical shifts are relative to 85% $H_3PO_4$. Molecular weights were determined (relative to polystyrene standard) on a Perkin–Elmer GPC equipped with a set of Waters Styragel columns (HT 6 200K-10M, HT 5 50K-4M, HT 4 5K-600K, HT 3 500K-30K), and a UV detector. Tetrahydrofuran (THF) (HPLC grade; Aldrich) was the eluent (flow rate: 1 ml min$^{-1}$). Mass spectra were obtained on a Fisons Instruments VG-Platform Benchtop LC-MS (positive ion electrospray mass spectra, ESP$^+$) spectrometer.

Solvents, including those used for NMR and chromatography, were thoroughly degassed before use. Chromatographic separations were performed with 70–230 mesh silica gel (Merck).

All manipulations were carried out with Schlenk type equipment under an atmosphere of argon on a dual manifold/argon-vacuum system. Liquids transferred by syringe or cannula. Solvents were dried (THF over sodium–potassium alloy, toluene and dioxane over sodium), and argon-saturated prior to use; DMF was distilled from $CaH_2$ under reduced pressure.

*trans*-$Pd(PBu)_3PdCl_2$ (**2**) [24,25] and *trans*-$Pt(PBu)_3PtCl_2$ (**3**) [25,26] were prepared according to published procedures. 1,4-Bis[(tributyltin)ethynyl]benzene (**13**) and 1,4-bis[(tributyltin)ethynyl]-2,5-di(octyloxy)benzene (**14**) were prepared following our previously described procedure [3a].

Other chemicals were purchased from Aldrich and used as received unless otherwise specified.

Legend for $^{13}$C-NMR spectra:

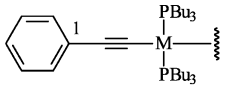


for **4**, **5**, **6** and **7**

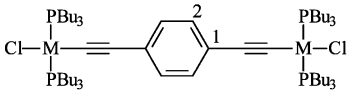


for **19** and **20**

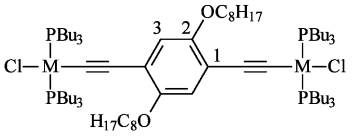


for **21** and **22**

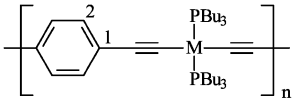


for **15** and **17**

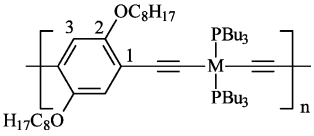


for **16** and **18**

### 4.2. Coupling of trans-dichlorobis(tributylphosphine)palladium(II) (2) with tributyl(phenylethynyl)tin

A Schlenk tube was loaded with *trans*-$(PBu_3)_2PdCl_2$ (**2**) (0.050 g, 0.086 mmol) and $Pd(PPh_3)_4$ (0.005 g, 0.004 mmol). After three cycles of vacuum/argon, were added by syringe $Bu_3SnC{\equiv}CPh$ (0.070 g, 0.17 mmol) and THF (20 ml). After 20 h stirring at 70 °C, $^{31}$P-NMR analysis showed the presence of two compounds, in addition to **2**. Approximately 10 g of Celite was added to the reaction mixture, and the solvent was removed under vacuum. The residue was chromatographed on alumina. After removal of $Bu_3SnCl$ by hexane, elution with hexane–benzene 9:1 produced a first band containing the unreacted complex **2** [25]. In spite of accuracy in executing the chromatographic separation, the second band eluted was a mixture of di- (**4**) and mono-substituted (**6**) products. A third fraction eluted and collected, after removal of the solvent, gave pure mono-substituted complex (**6**).

#### 4.2.1. trans-[Pd(PBu$_3$)$_2$(C≡C–C$_6$H$_5$)$_2$] (4)

$^{13}$C-NMR ($CDCl_3$): $\delta$ 13.8 (–$CH_3$), 22.8 (dd, $J_{C-P}$ = 13.6 Hz), 24.5 (dd, $J_{C-P}$ = 6.8 Hz), 26.6 (br) (P–($CH_2$)$_3$–), 111.8 (t, $J_{C-P}$ = 17.0 Hz, –$C$≡C–Ph), 113.4 (–C ≡ $C$–Ph), 124.9, 128.0 (*Ar*), 128.6 ($C_1$), 130.7 (*Ar*). $^{31}$P-NMR ($CDCl_3$): $\delta$ 11.2. MS (15 V, ESP$^+$): 510 (M + H − $PBu_3$)$^+$. Spectroscopic properties are in agreement with reported data [27].

#### 4.2.2. trans-[PdCl(PBu$_3$)$_2$(C≡C–C$_6$H$_5$)] (6)

$^1$H-NMR ($CDCl_3$): $\delta$ 0.90 (t, $J$ = 7.0 Hz, 18H, –C$H_3$), 1.42 (sx, $J$ = 7.0 Hz, 12H, –$CH_2$–C$H_2$–$CH_3$), 1.55 (m, 12H, –C$H_2$–$CH_2$–$CH_3$), 1.91 (m, 12H, PC$H_2$–), 7.08–7.25 (m, 5H, Ar–*H*). $^{13}$C-NMR ($CDCl_3$): $\delta$ 13.7 (–$CH_3$), 22.8 (dd, $J_{C-P}$ = 13.6 Hz), 24.3 (dd, $J_{C-P}$ = 6.8 Hz), 26.3 (dd, $J_{C-P}$ = 18.1 Hz) (P–($CH_2$)$_3$–), 96.2 (t, $J_{C-P}$ = 15.8 Hz, –$C$≡C–Ph), 105.7 (t, $J_{C-P}$ = 5.7 Hz, –C≡$C$–Ph), 125.4, 127.9 (*Ar*), 128.3 ($C_1$), 130.5 (*Ar*). $^{31}$P-NMR ($CDCl_3$): $\delta$ 10.4. IR ($CH_2Cl_2$, cm$^{-1}$): 2963 (s), 2932 (s), 2903 (w), 2874 (s), 2116 (s) ($\nu_{C\equiv C}$), 1595 (m), 1485 (m), 1465 (m), 1411 (w), 1379 (w), 1343 (w), 1304 (w). $\lambda_{max}$ ($CH_2Cl_2$): 273 nm. Anal. Calc. for $C_{32}H_{59}ClP_2Pd$: C, 59.35; H, 9.18. Found: C, 59.27; H, 9.27%. MS (15 V, ESP$^+$): 653 (M + Li)$^+$, 612 (M − Cl)$^+$. Spectroscopic and analytical properties are in agreement with reported data [28].

### 4.3. Coupling of trans-dichlorobis(tributylphosphine)platinum(II) (3) with tributyl(phenylethynyl)tin

A Schlenk tube was loaded with *trans*-$Pt(PBu_3)_2PtCl_2$ (**3**) (0.050 g, 0.075 mmol) and $Pd(PPh_3)_4$ (0.005 g, 0.004 mmol). After three cycles of vacuum/argon, were added by syringe $Bu_3SnC{\equiv}CPh$ (0.058 g, 0.15 mmol) and THF (20 ml). After 20 h stirring at 70 °C, $^{31}$P-NMR analysis showed the presence of two compounds, in addition to **3**. Approximately 10 g of Celite was added to the reaction mixture, and the solvent was removed under vacuum. The residue was chromatographed on a silica gel column. After removal of $Bu_3SnCl$ by hexane, elution with hexane–dichlorometane 9:1 produced a first band containing the unreacted complex **3** [25]. Then, further elution with the same solvent mixture

allowed the separation of a second and a third bands, which were collected and, after removal of the solvent, gave di- (**5**) and mono-substituted (**7**) products, respectively.

#### 4.3.1. trans-[Pt(PBu$_3$)$_2$(C≡C–C$_6$H$_5$)$_2$] (5)

$^1$H-NMR ($CDCl_3$): $\delta$ 0.91 (t, $J = 7.3$ Hz, 18H, –C$H_3$), 1.43 (sx, $J = 7.0$ Hz, 12H, –CH$_2$–C$H_2$–CH$_3$), 1.59 (m, 12H, –C$H_2$–CH$_2$–CH$_3$), 2.12 (m, 12H, PC$H_2$–), 7.06–7.27 (m, 10H, Ar–*H*). $^{13}$C-NMR ($CDCl_3$): $\delta$ 13.8 (–*C*H$_3$), 23.9 (dd, $J_{C-P} = 16.2$, 18.0 Hz), 24.4 (dd, $J_{C-P} = 5.4$, 7.2 Hz), 26.6 (dd, $J_{C-P} = 10.8$, 12.6 Hz) (P–(*C*H$_2$)$_3$–), 108.0 (t, $J_{C-P} = 14.4$ Hz, –*C*≡C–Ph), 108.8 (–C≡*C*–Ph), 124.7, 127.8 (*Ar*), 129.1 ($C_1$), 130.7 (*Ar*). $^{31}$P-NMR ($CDCl_3$): $\delta$ 3.7 ($J_{P-Pt} = 2359$ Hz). IR ($CH_2Cl_2$, cm$^{-1}$): 2964 (s), 2934 (s), 2903 (w), 2873 (s), 2101 (s) ($\nu_{C\equiv C}$), 1593 (m), 1485 (m), 1465 (m), 1379 (w). $\lambda_{max}$ ($CH_2Cl_2$): 327 nm. Anal. Calc. for $C_{40}H_{64}P_2Pt$: C, 59.91; H, 8.04. Found: C, 59.76; H, 8.07%. MS (15 V, ESP$^+$): 803 (M+H)$^+$. Spectroscopic and analytical properties are in agreement with reported data [27,29].

#### 4.3.2. trans-[PtCl(PBu$_3$)$_2$(C≡C–C$_6$H$_5$)] (7)

$^1$H-NMR ($CDCl_3$): $\delta$ 0.91 (t, $J = 7.2$ Hz, 18H, –C$H_3$), 1.45 (sx, $J = 7.2$ Hz, 12H, –CH$_2$–C$H_2$–CH$_3$), 1.60 (m, 12H, –C$H_2$–CH$_2$–CH$_3$), 1.99 (m, 12H, PC$H_2$–), 7.07–7.28 (m, 5H, Ar–*H*) $^{13}$C-NMR ($CDCl_3$): $\delta$ 13.8 (–*C*H$_3$), 21.9 (dd, $J_{C-P} = 16.2$, 18.0 Hz), 24.3 (dd, $J_{C-P} = 5.4$, 7.2 Hz), 26.0 (dd, $J_{C-P} = 9.0$, 10.8 Hz) (P–(*C*H$_2$)$_3$–), 82.9 (t, $J_{C-P} = 14.6$ Hz, –*C*≡C–Ph), 101.0 (t, $J_{C-P} = 2.4$ Hz, –C≡*C*–Ph), 125.0, 127.9 (*Ar*), 128.9 ($C_1$), 130.7 (*Ar*). $^{31}$P-NMR ($CDCl_3$): $\delta$ 7.5 ($J_{P-Pt} = 2373$ Hz). IR ($CH_2Cl_2$, cm$^{-1}$): 2964 (s), 2933 (s), 2933 (s), 2874 (s), 2119 (s) ($\nu_{C\equiv C}$), 1593 (m). $\lambda_{max}$ ($CH_2Cl_2$): 287 nm. Anal. Calc. for $C_{32}H_{59}ClP_2Pt$: C, 52.20; H, 8.08. Found: C, 52.38; H, 8.28%. MS (15 V, ESP$^+$): *742* (M+Li)$^+$. Spectroscopic and analytical properties are in agreement with reported data [30].

### 4.4. Characterization of bimetallic complexes

#### 4.4.1. trans-1,4-[PdCl(PBu$_3$)$_2$C≡C]$_2$C$_6$H$_4$ (19)

Pale yellow needles crystals. $^1$H-NMR ($CDCl_3$): $\delta$ 0.89 (t, $J = 7.0$ Hz, 36H, –C$H_3$), 1.41 (sx, $J = 7.0$ Hz, 24H, –CH$_2$–C$H_2$–CH$_3$), 1.54 (m, 24H, –C$H_2$–CH$_2$–CH$_3$), 1.90 (br, 24H, P–C$H_2$–), 7.07 (s, 4H, Ar–*H*). $^{13}$C-NMR ($CDCl_3$): $\delta$ 13.5 (–*C*H$_3$), 22.5 (dd, $J_{C-P} = 13.6$ Hz), 24.1 (dd, $J_{C-P} = 6.8$ Hz), 26.1 (P–(*C*H$_2$)$_3$–), 96.7 (t, $J_{C-P} = 15.8$ Hz, –C≡*C*–Pd–), 105.7 (t, $J_{C-P} = 5.7$ Hz, –*C*≡C–Pd–), 124.7 ($C_1$), 129.9 ($C_2$). $^{31}$P-NMR ($CDCl_3$): $\delta$ 10.4. IR ($CH_2Cl_2$, cm$^{-1}$): 2971 (s), 2941 (w), 2879 (s), 2836 (m), 2686 (s), 2306 (s), 2115 (m) ($\nu_{C\equiv C}$), 1464 (w), 1420 (w), 1379 (w). $\lambda_{max}$ ($CH_2Cl_2$): 308 nm. Anal. Calc. for $C_{58}H_{112}Cl_2P_4Pd_2$: C, 57.23; H, 9.27. Found: C, 57.32; H, 9.43%. Spectroscopic and analytical properties are in agreement with reported data [31].

#### 4.4.2. trans-1,4-[PdCl(PBu$_3$)$_2$C≡C]$_2$C$_6$H$_2$-2,5-(OC$_8$H$_{17}$)$_2$ (21)

Dark orange needles crystals. $^1$H-NMR ($CDCl_3$): $\delta$ 0.88 (t, $J = 7.1$ Hz, 36H, P(CH$_2$)$_3$–C$H_3$), 0.89 (t, $J = 7.6$ Hz, 6H, –O(CH$_2$)$_7$–C$H_3$), 1.21–1.72 (m, 72H, P–CH$_2$–(C$H_2$)$_2$–CH$_3$ + –OCH$_2$–(C$H_2$)$_6$–CH$_3$), 1.92 (m, 24H, P–C$H_2$–), 3.83 (t, $J = 6.7$ Hz, 4H, –O–C$H_2$–), 6.65 (s, 2H, Ar–*H*). $^{13}$C-NMR ($CDCl_3$): $\delta$ 13.7 (P(CH$_2$)$_3$*C*H$_3$), 13.9 (–OCH$_2$–(CH$_2$)$_6$–*C*H$_3$), 22.6 (dd, $J_{C-P} = 12.6$, 14.4 Hz, P–(*C*H$_2$)$_3$– + –OCH$_2$–(*C*H$_2$)$_6$–CH$_3$), 24.3 (dd, $J_{C-P} = 7.2$ Hz, P–(*C*H$_2$)$_3$–), 25.9 (–OCH$_2$–(*C*H$_2$)$_6$–CH$_3$), 26.3 (P–(*C*H$_2$)$_3$–), 29.2, 29.4, 29.5, 31.7 (–OCH$_2$–(*C*H$_2$)$_6$–CH$_3$), 69.0 (–O–*C*H$_2$–), 100.3 (t, $J_{C-P} = 16.2$ Hz, –C≡*C*–Pd–), 101.8 (t, $J_{C-P} = 5.4$ Hz, –*C*≡C–Pd–), 115.3 ($C_1$), 116.8 ($C_3$), 152.6 ($C_2$). $^{31}$P-NMR ($CDCl_3$): $\delta$ 10.3. IR ($CH_2Cl_2$, cm$^{-1}$): 2973 (s), 2946 (s), 2884 (s), 2842 (m), 2864 (s), 2305 (s), 2110 (m) ($\nu_{C\equiv C}$), 1494 (m), 1466 (m), 1379 (w). $\lambda_{max}$ ($CH_2Cl_2$): 344 nm. Anal. Calc. for $C_{72}H_{144}Cl_2O_2P_4Pd_2$: C, 60.32; H, 9.85. Found: C, 60.56; H, 10.11%.

#### 4.4.3. trans-1,4-[PtCl(PBu$_3$)$_2$C≡C]$_2$C$_6$H$_4$ (20)

Yellow crystalline solid. $^1$H-NMR ($CDCl_3$): $\delta$ 0.89 (t, $J = 7.0$ Hz, 36H, –C$H_3$), 1.41 (sx, $J = 7.0$ Hz, 24H, –CH$_2$–C$H_2$–CH$_3$), 1.54 (m, 24H, –C$H_2$–CH$_2$–CH$_3$), 1.97 (m, 24H, P–C$H_2$–), 7.05 (s, 4H, Ar–*H*). $^{13}$C-NMR ($CDCl_3$): $\delta$ 13.7 (–*C*H$_3$), 21.9 (dd, $J_{C-P} = 17.1$ Hz), 24.3 (dd, $J_{C-P} = 6.1$, 7.3 Hz), 26.1 (P–(*C*H$_2$)$_3$–), 83.5 (t, $J_{C-P} = 14.6$ Hz, –C≡*C*–Pt–), 101.3 (t, $J_{C-P} = 2.4$ Hz, –*C*≡C–Pt–), 125.6 ($C_1$), 130.3 ($C_2$). $^{31}$P-NMR ($CDCl_3$): $\delta$ 7.4 ($J_{P-Pt} = 2366$ Hz). IR ($CH_2Cl_2$, cm$^{-1}$): 2964 (s), 2933 (s), 2875 (s), 2119 (s) ($\nu_{C\equiv C}$), 1499 (m), 1465 (m). $\lambda_{max}$ ($CH_2Cl_2$): 348 nm. Anal. Calc. for $C_{58}H_{112}Cl_2P_4Pt_2$: C, 49.96; H, 8.10. Found: C, 49.78; H, 8.20%. Spectroscopic and analytical properties are in agreement with reported data [31,32].

#### 4.4.4. trans-1,4-[PtCl(PBu$_3$)$_2$C≡C]$_2$C$_6$H$_2$-2,5-(OC$_8$H$_{17}$)$_2$ (22)

Yellow crystalline solid. $^1$H-NMR ($CDCl_3$): $\delta$ 0.88 (t, $J = 7.0$ Hz, 42H, P(CH$_2$)$_3$–C$H_3$ + –O(CH$_2$)$_7$–C$H_3$), 1.23–1.74 (m, 72H, P–CH$_2$–(C$H_2$)$_2$–CH$_3$ + –OCH$_2$–(C$H_2$)$_6$–CH$_3$), 2.01 (m, 24H, P–C$H_2$–), 3.83 (t, $J = 7.0$ Hz, 4H, –O–C$H_2$–), 6.64 (s, 2H, Ar–*H*). $^{13}$C-NMR ($CDCl_3$): $\delta$ 13.8 (P(CH$_2$)$_3$*C*H$_3$), 14.1 (–OCH$_2$–(CH$_2$)$_6$–*C*H$_3$), 21.8 (dd, $J_{C-P} = 17.0$ Hz, P–(*C*H$_2$)$_3$–), 22.7 (–OCH$_2$–(*C*H$_2$)$_6$–CH$_3$), 24.3 (dd, $J_{C-P} = 6.8$ Hz, P–(*C*H$_2$)$_3$–), 26.0 (–OCH$_2$–(*C*H$_2$)$_6$–CH$_3$), 26.1 (P–(*C*H$_2$)$_3$–), 29.3, 29.5, 29.7, 31.9 (–OCH$_2$–(*C*H$_2$)$_6$–CH$_3$), 69.1 (–O–*C*H$_2$–), 86.4 (t, $J_{C-P} = 15.8$ Hz, –C≡*C*–Pt–), 97.2 (t, $J_{C-P} = 2.3$ Hz, –*C*≡C–Pt–), 116.0 ($C_1$), 117.0 ($C_3$), 152.9 ($C_2$). $^{31}$P-NMR ($CDCl_3$): $\delta$ 7.6 ($J_{P-Pt} = 2368$ Hz) IR ($CH_2Cl_2$, cm$^{-1}$): 2963 (s), 2933 (s),

2874 (s), 2114 (m) ($\nu_{C\equiv C}$), 1606 (m), 1494 (m), 1466 (m). $\lambda_{max}$ ($CH_2Cl_2$): 395 nm. Anal. Calc. for $C_{74}H_{144}Cl_2O_2P_4Pt_2$: C, 53.84; H, 8.79. Found: C, 53.51; H, 8.72%.

### 4.5. General preparation of polymers

A Schlenk tube was loaded with the metal complexes **2** or **3** and an equivalent amount of the distannyl compounds **13** or **14**. After three cycles of vacuum/argon, solvent (dioxane for palladium complex **2** and toluene for platinum complex **3**) was added by syringe. The reaction mixture was heated to reflux for several hours (70 °C, 8 h for **2** in dioxane, 110 °C, 26 h for **3** in toluene). After cooling to room temperature, the reaction mixture was concentrated to a minimum volume, and then diluted with methanol until a solid precipitate was obtained, which was washed repeatedly with methanol and dried under vacuum.

Table 4
Crystal data and structure refinement

| Identification code | **19** | **21** |
|---|---|---|
| Empirical formula | $C_{58}H_{112}Cl_2P_4Pd_2$ | $C_{74}H_{144}Cl_2O_2P_4Pt_2$ |
| Formula weight | 1217.06 | 1473.47 |
| Temperature (K) | 293(2) | 293(2) |
| Wavelength (Å) | 1.54180 | 0.71073 |
| Crystal system | Monoclinic | Triclinic |
| Space group | $C2/c$ | $P\bar{1}$ |
| Unit cell dimensions | | |
| $a$ (Å) | 35.332(5) | 12.228(6) |
| $b$ (Å) | 16.502(7) | 12.960(2) |
| $c$ (Å) | 13.006(3) | 15.898(2) |
| $\alpha$ (°) | | 101.048(12) |
| $\beta$ (°) | 113.16(3) | 99.05(2) |
| $\gamma$ (°) | | 113.791(17) |
| $V$ (Å$^3$) | 6972(4) | 2184.0(12) |
| Z | 4 | 1 |
| $D_{calc}$ (g cm$^{-3}$) | 1.159 | 1.120 |
| Absorption coefficient (mm$^{-1}$) | 5.949 | 0.582 |
| $F$(000) | 2584 | 790 |
| Crystal size (mm$^3$) | 0.50 × 0.50 × 0.08 | 0.60 × 0.45 × 0.08 |
| $\theta$ Range for data collection (°) | 2.72–55.07 | 2.01–22.97 |
| Index ranges | $-37 \le h \le 37$, $-13 \le k \le 2$ $-17 \le l \le 17$ | $-13 \le h \le 13$, $-14 \le k \le 13$, $-0 \le l \le 17$ |
| Reflections collected | 8714 | 6045 |
| Independent reflections | 4386 [$R_{int} = 0.3405$] | 6045 [$R_{int} = 0.0000$] |
| Completeness to $\theta = 55.07°$ | 100.0% | 99.7% |
| Max/min transmission | 0.6639/0.1549 | 0.9576/0.7213 |
| Refinement method | Full-matrix least-squares on $F^2$ | |
| Data/restraints/parameters | 4386/0/145 | 6045/39/222 |
| Goodness-of-fit on $F^2$ | 1.347 | 1.013 |
| Final $R$ indices [$I > 2\sigma(I)$] | $R_1 = 0.2076$, $wR_2 = 0.4718$ | $R_1 = 0.0741$, $wR_2 = 0.1844$ |
| $R$ indices (all data) | $R_1 = 0.2913$, $wR_2 = 0.5342$ | $R_1 = 0.1430$, $wR_2 = 0.2235$ |
| Largest difference peak and hole (e Å$^{-3}$) | 1.387 and −0.771 | 0.686 and −0.4553 |

#### 4.5.1. trans-1,4-[Pd(PBu$_3$)$_2$–C≡C–C$_6$H$_4$–C≡C]$_n$ (**15**)

Coffee-brown solid. $^1$H-NMR ($CDCl_3$): $\delta$ 0.89 (br, 18H, –C$H_3$), 1.42 (br, 12H, –CH$_2$–C$H_2$–CH$_3$), 1.54 (br, 12H, –C$H_2$–CH$_2$–CH$_3$), 1.90 (br, 12H, PC$H_2$–), 7.07 (br, 4H, Ar–$H$). $^{13}$C-NMR ($CDCl_3$): $\delta$ 13.8 (–$C$H$_3$), 22.8, 24.4, 26.4 (P–($C$H$_2$)$_3$–), 106.1 (–$C$≡$C$–), 131.2 (m, $Ar$). $^{31}$P-NMR ($CDCl_3$): $\delta$ 10.6 (br). IR ($CH_2Cl_2$, cm$^{-1}$): 2970 (w), 2943 (w), 2885 (w), 2843 (w), 2304 (s), 2112 (w) ($\nu_{C\equiv C}$), 1598 (w), 1464 (w), 1414 (w), 1379 (w). $\lambda_{max}$ ($CH_2Cl_2$): 315 nm. Spectroscopic and analytical properties are in agreement with reported data [31,33].

#### 4.5.2. trans-1,4-[Pd(PBu$_3$)$_2$–C≡C–C$_6$H$_2$(2,5-(OC$_8$H$_{17}$)$_2$)–C≡C]$_n$ (**16**)

Dark brown sticky oil. $^1$H-NMR ($CDCl_3$): $\delta$ 0.86 (br, 24H, P(CH$_2$)$_3$–C$H_3$ + –O(CH$_2$)$_7$–C$H_3$), 1.26–2.03 (m, 60H, P(C$H_2$)$_3$CH$_3$ + –OCH$_2$(C$H_2$)$_6$CH$_3$), 3.85 (br, 4H, –O–C$H_2$–), 6.70 (br, 2H, Ar–$H$). $^{13}$C-NMR ($CDCl_3$): $\delta$ 13.9 (P(CH$_2$)$_3$$C$H$_3$), 14.1 (–OCH$_2$–(CH$_2$)$_6$–$C$H$_3$), 22.7–31.9 (P–($C$H$_2$)$_3$–CH$_3$ + –OCH$_2$–($C$H$_2$)$_6$–CH$_3$), 69.1 (–O–$C$H$_2$–), 106.6 (–$C$≡$C$–), 115.8 ($C_1$), 117.4 ($C_3$), 152.7 ($C_2$). $^{31}$P-NMR ($CDCl_3$): $\delta$ 10.3 (br, terminal), 11.3 (br, internal). IR ($CH_2Cl_2$, cm$^{-1}$): 2882 (w), 2845 (w), 2684 (s), 2305 (s), 2097 (w) ($\nu_{C\equiv C}$), 1605 (m), 1493 (w), 1467 (w). $\lambda_{max}$ ($CH_2Cl_2$): 374 nm.

#### 4.5.3. trans-1,4-[Pt(PBu$_3$)$_2$–C≡C–C$_6$H$_4$–C≡C]$_n$ (**17**)

Yellow–brown solid. $^1$H-NMR ($CDCl_3$): $\delta$ 0.89 (br, 18H, –C$H_3$), 1.42 (br, 12H, –CH$_2$–C$H_2$–CH$_3$), 1.56 (br, 12H, –C$H_2$–CH$_2$–CH$_3$), 2.10 (br, 12H, PC$H_2$–), 7.07 (br, 4H, Ar–$H$). $^{13}$C-NMR ($CDCl_3$): $\delta$ 13.8 (–$C$H$_3$), 23.9 (dd, $J_{C-P} = 18.0$ Hz, $J_{C-P} = 16.2$ Hz), 24.4 (dd, $J_{C-P} = 7.2$ Hz), 26.3 (P($C$H$_2$)$_3$CH$_3$), 109.4 (–$C$≡$C$–), 125.5 ($C_1$), 130.3 ($C_2$). $^{31}$P-NMR ($CDCl_3$): $\delta$ 3.5 ($J_{P-Pt} = 2355$ Hz, internal), 7.4 ($J_{P-Pt} = 2366$ Hz, terminal). IR ($CH_2Cl_2$, cm$^{-1}$): 2964 (s), 2933 (s), 2874 (s), 2098 (s) ($\nu_{C\equiv C}$), 1597 (m), 1499 (m), 1465 (m). $\lambda_{max}$ ($CH_2Cl_2$): 364 nm. Spectroscopic and analytical properties are in agreement with reported data [32b,34].

#### 4.5.4. trans-1,4-[Pt(PBu$_3$)$_2$–C≡C–C$_6$H$_2$(2,5-(OC$_8$H$_{17}$)$_2$)–C≡C]$_n$ (**18**)

Dark brown sticky oil. $^1$H-NMR ($CDCl_3$): $\delta$ 0.89 (br, 24H, P(CH$_2$)$_3$–C$H_3$ + –O(CH$_2$)$_7$–C$H_3$), 1.23–2.21 (m, 60H, P(C$H_2$)$_3$CH$_3$ + –OCH$_2$(C$H_2$)$_6$CH$_3$), 3.85 (br, 4H, –O–C$H_2$–), 6.64, 6.68 (Ar–$H$). $^{13}$C-NMR ($CDCl_3$): $\delta$ 13.8 (P(CH$_2$)$_3$$C$H$_3$), 14.0 (–OCH$_2$–(CH$_2$)$_6$–$C$H$_3$), 21.5–31.9 (P–($C$H$_2$)$_3$–CH$_3$ + –OCH$_2$–($C$H$_2$)$_6$–CH$_3$),

69.1 (–O–$CH_2$–), 97.3, 105.3 (–$C$≡$C$–), 117.0 ($C_1$), 117.1 ($C_3$), 152.9 ($C_2$). $^{31}$P-NMR ($CDCl_3$): $\delta$ 3.9 ($J_{P-Pt}$ = 2364 Hz, internal), 7.6 ($J_{P-Pt}$ = 2368 Hz, terminal). IR ($CH_2Cl_2$, $cm^{-1}$): 2965 (s), 2935 (s), 2875 (s), 2096 (s) ($\nu_{C\equiv C}$), 1494 (m), 1466 (m). $\lambda_{max}$ ($CH_2Cl_2$): 395 nm.

### 4.6. X-ray diffraction studies

A summary of crystal and intensity data for compounds **19** and **21** is presented in Table 4.

For compound **19** the low resolution does not allow detailed discussion of structural parameters, however, there is no doubt about the overall geometry and atomic connectivity. For compound **21**, experimental data were recorded at room temperature (20 °C) on an Enraf–Nonius CAD4. A set of 25 carefully cantered reflections in the range $7° < \theta < 9°$ was used for determining the lattice constants. As a general procedure, the intensity of three standard reflections were measured periodically every 200 reflections for orientation and intensity control. This procedure did not reveal decay of intensities. The data were corrected for Lp. Atomic scattering factors were those taken from Ref. [35] with anomalous dispersion corrections taken from Ref. [36]. The computational work was carried out by intensively using the program SHELX-97 [37].

Final atomic co-ordinates of all atoms and structure factors are available on request from the authors and are provided as supplementary material.

A pale yellow parallelepiped crystal with dimension 0.6 × 0.45 × 0.075 mm was used for the data collection. The structure was solved by direct methods using the SIR-97 program [38].

Refinement was done by full-matrix least-squares calculations, initially with isotropic thermal parameters then with anisotropic thermal parameters for Pd, Cl, O, P and C atoms of the phenyl ring and the C atoms that are linked to the Pd atom. The hydrogen atoms were introduced at calculated positions. An absorption correction was applied using the program XABS-2 [39].

## 5. Supplementary material

Crystallographic data for the structural analysis have been deposited with the Cambridge Crystallographic Data Centre, CCDC nos. 215521 and 215522 for compounds **19** and **21**. Copies of this information may be obtained free of charge from The Director, CCDC, 12 Union Road, Cambridge CB2 1EZ, UK (Fax: +44-1223-336033; e-mail: deposit@ccdc.cam.ac.uk or www: http://www.ccdc.cam.ac.uk).

## Acknowledgements

This work was supported by the Consiglio Nazionale delle Ricerche (C.N.R. Roma), with the 'Progetto Finalizzato C.N.R.-Materiali Speciali per Tecnologie Avanzate II', contract no. 97.00946.PF34, and the 'Progetto Finalizzato C.N.R.-Materiali e Dispositivi per l'Elettronica a Stato Solido', contract no. 97.01350.PF48.

## References

[1] (a) T.A. Skotheim, R.L. Elsenbaumer, J.R. Reynolds, Handbook of Conducting Polymers, 2nd ed., Marcel Dekker, Inc, New York, 1998;
(b) W.J. Blau, P. Lianos, U. Schubert, Molecular Materials and Functional Polymers, Springer Wien, New York, 2001;
(c) U.H.F. Bunz, Chem. Rev. 100 (2000) 1605–1644;
(d) P.F. Schwab, M.D. Lewin, J. Michl, Chem. Rev. 99 (1999) 1863–1934;
(e) J.C. Ellenbogen, J.C. Love, Proceedings of the IEEE, vol. 88, No.3, 2000.;
(f) T. Yamamoto, Synlett 4 (2003) 425.

[2] (a) S. Takahashi, Y. Takai, H. Morimoto, K. Sonogashira, N. Hagihara, Mol. Cryst. Liq. Cryst. 32 (1982) 139;
(b) D. Posselt, W. Badur, M. Steiner, M. Baumgarten, Synth. Met. 55–57 (1993) 3299;
(c) M. Hmyene, A. Yassar, M. Escorne, A. Percheron-Guegan, F. Garnier, Adv. Mater. 6 (1994) 564;
(d) W.J. Blau, H.J. Byrne, D.J. Cardin, A.P. Davey, J. Mater. Chem. 1 (1991) 245;
(e) N.J. Long, Angew. Chem. Int. Ed. Engl. 34 (1995) 21;
(f) H. Lang, Angew. Chem. Int. Ed. Engl. 33 (1994) 547.

[3] (a) E. Antonelli, P. Rosi, C. Lo Sterzo, E. Viola, J. Organomet. Chem. 578 (1999) 210;
(b) R. Pizzoferrato, M. Berliocchi, A. Di Carlo, P. Lugli, M. Venanzi, A. Micozzi, A. Ricci, C. Lo Sterzo, Macromolecules 36 (2003) 2215.

[4] M. Ottaviani, A. Micozzi, C. Lo Sterzo, Manuscript in preparation.

[5] C. Lo Sterzo, Synlett 11 (1999) 1704.

[6] (a) E. Viola, C. Lo Sterzo, F. Trezzi, Organometallics 15 (1996) 4352;
(b) A. Buttinelli, E. Viola, E. Antonelli, C. Lo Sterzo, Organometallics 17 (1998) 2574.

[7] (a) P. Altamura, G. Giardina, C. Lo Sterzo, M.V. Russo, Organometallics 20 (2001) 4360;
(b) C. Caliendo, I. Fratoddi, M.V. Russo, C. Lo Sterzo, J. Appl. Phys. 93 (2003) 10071.

[8] (a) K. Osakada, T. Yamamoto, Rev. Heteroatom Chem. 21 (1999) 163;
(b) K. Osakada, T. Yamamoto, Coord. Chem. Rev. 198 (2000) 379;
(c) A. Ricci, F. Angelucci, M. Bassetti, C. Lo Sterzo, J. Am. Chem. Soc. 124 (2002) 1060.

[9] Tipically a reaction mixture containing both mono- and di-substituted products **6** and **4** or **7** and **5** was submitted to chromatographic separation, and, after isolation single components were identified by spectroscopic and microanalytical data (see Section 4).

[10] As an example in the reaction of **2** and **1** in absence of $Pd(PPh_3)_4$ (DMF, 25 °C), **6** (85%) and **2** (15%) were present after 20 h. After addition of 5% of $Pd(PPh_3)_4$, **6** and **2** amounted at 70 and 30%,

respectively, after 20 h, 50 and 50%, respectively, after 40 h, and 25 and 75%, respectively, after 60 h at 25 °C.

[11] I. Fratoddi, C. Battocchio, A. Furlani, P. Mataloni, G. Polzonetti, M.V. Russo, J. Organomet. Chem. 674 (2003) 10.

[12] Y. Zhu, D.B. Millet, M.O. Wolf, S.J. Rettig, Organometallics 18 (1999) 1930.

[13] (a) S.J. Davies, B.F.G. Johnson, M.S. Kan, J. Lewis, J. Chem. Soc. Chem. Commun. (1991) 187;
(b) S.J. Davies, B.F.G. Johnson, M.S. Kan, J. Lewis, J. Organomet. Chem. 401 (1991) C43;
(c) B.F.G. Johnson, A.K. Kakkar, M.S. Kan, J. Lewis, J. Organomet. Chem. 409 (1991) C12;
(d) B.F.G. Johnson, A.K. Kakkar, M.S. Kan, J. Lewis, A.E. Dray, R.H. Friend, F. Wittmann, J. Mater. Chem. 1 (1991) 485;
(e) Z. Atherton, C.W. Faulkner, S.L. Ingham, A.K. Kakkar, M.S. Kan, J. Lewis, N.J. Long, R.P. Raithby, J. Organomet. Chem. 462 (1993) 265;
(f) W.A. Herrmann, Synthetic Methods of Organometallic and Inorganic Chemistry, vol. 7 (Chapter 5), Thieme, New York, 1997 (Chapter 5).

[14] $^{31}$P-NMR spectrum of **17b** displayed a 1:4.8 terminal vs internal signal ratio, accounting for a polymer chain length of 12 units.

[15] (a) J. Lewis, N.J. Long, P.R. Raithby, G.P. Shields, W.Y. Wong, M. Younus, J. Chem. Soc. Dalton Trans. (1997) 4283;
(b) W.Y. Wong, W.K. Wong, P.R. Raithby, J. Chem. Soc. Dalton Trans. (1998) 2761.

[16] (a) U. Behrens, K. Hoffmann, J. Organomet. Chem. 129 (1977) 273;
(b) K. Onitsuka, H. Ogawa, T. Joh, S. Takahashi, Y. Yamamoto, H. Yamazaki, J. Chem. Soc. Dalton Trans. (1991) 1531;
(c) K. Onitsuka, S. Yamamoto, S. Takahashi, Angew. Chem. Int. Ed. 38 (1999) 174.

[17] In **19**, because of the large thermal motion, is not possible to give a reliable value for the same structural characteristic.

[18] (a) W.Y. Wong, S.-M. Chan, K.-H. Choi, K.-W. Cheah, W.-K. Chan, Macromol. Rapid Commun. (2000) 453;
(b) W.Y. Wong, G.-L. Lu, K.-H. Choi, J.-X. Shi, Macromolecules 35 (2002) 3506.

[19] (a) D. Ofer, T.M. Swager, M.S. Wrighton, Chem. Mater. 7 (1995) 418;
(b) U.H.F. Bunz, V. Enkelmann, L. Kloppenburg, D. Jones, K.D. Shimizu, J.B. Claridge, H.-C. zur Loye, G. Lieser, Chem. Mater. 11 (1999) 1416.

[20] (a) M.L. Renach, G.P. Bartholomew, S. Wang, P.J. Ricatto, R.J. Lachicotte, G.C. Bazan, J. Am. Chem. Soc. 121 (1999) 7787;
(b) T. Miteva, L. Palmer, L. Kloppenburg, D. Neher, U.H.F. Bunz, Macromolecules 33 (2000) 652.

[21] P. Samorì, V. Francke, K. Müllen, J.P. Rabe, Chem. Eur. J. 5 (8) (1999) 2312.

[22] (a) D. Ofer, T.M. Swager, M. Wrighton, Chem. Mater. 7 (1995) 418;
(b) P. Wautelet, M. Moroni, L. Oswald, J. Le Moine, T.A. Pham, J.-Y. Bigot, Macromolecules 29 (1996) 446;
(c) M. Moroni, J. Le Moine, T.A. Pham, J.-Y. Bigot, Macromolecules 30 (1997) 1964;
(d) C. Weder, M. Wrighton, Macromolecules 29 (1996) 5157.

[23] (a) D.L. Pearson, J.S. Schumm, J.M. Tour, Macromolecules 27 (1994) 2348;
(b) J.M. Tour, Chem. Rev. 96 (1996) 537;
(c) See Ref. [22] inside Ref. [7a].

[24] T. Saito, H. Munakata, H. Imoto, Inorg. Synth. 17 (1977) 83.

[25] P.S. Pregosin, R.W. Kunz, $^{31}$P- and $^{13}$C-NMR of Transition Metal Complexes (NMR Basic Princ. Prog. (1979) 16).

[26] B. Kauffman, L.A. Teter, J.E. Huheey, Inorg. Synth. 7 (1963) 245.

[27] A. Sebald, B. Wrackmeyer, W. Beck, Z. Naturforsch., B; Inorg. Chem., Org. Chem. 38B (1) (1983) 45–56.

[28] S.-M. Kuang, Z.-Z. Zhang, Q.-G. Wang, T.C.W. Mak, J. Chem. Soc. Dalton Trans. Inorg. Chem. 7 (1998) 1115.

[29] J.E. Rogers, T.M. Cooper, P.A. Fleitz, D.J. Glass, D.G. McLean, J. Phys. Chem. A 106 (2002) 10108.

[30] S. Miki, T. Ohno, H. Iwasaki, Z. Yoshida, J. Phys. Org. Chem. 1 (6) (1988) 333.

[31] M.S. Khan, S.J. Davies, A.K. Kakkar, D. Schwartz, B. Lin, B.F.G. Johnson, J. Lewis, J. Organomet. Chem. 424 (1992) 87.

[32] (a) S. Takahashi, Y. Ohyama, E. Murata, K. Sonogashira, N. Hagihara, J Polym. Sci. Polym. Chem. Ed. 18 (1980) 349;
(b) M.I. Bruce, J. Davy, B.C. Hall, Y. Jansen van Galen, B.W. Skelton, A.H. White, Appl. Organomet. Chem. 16 (2002) 559.

[33] S. Takahashi, H. Morimoto, E. Murata, S. Kataoka, K. Sonogashira, N. Hagihara, J Polym. Sci. Polym. Chem. Ed. 20 (1982) 565.

[34] S. Takahashi, M. Kariya, T. Yatake, K. Sonogashira, N. Hagihara, Macromolecules 11 (6) (1978) 1978.

[35] D.T. Cromer, J.T. Waber, Acta Crystallogr. 18 (1965) 104.

[36] International Tables of Crystallography, vol. IV, Kynoch Press, Birmingham, UK, 1974.

[37] G.M. Sheldrick, SHELX-97, Program for Structure Refinement, University of Göttingen, Germany, Release 97-21997.

[38] A. Altomare, M.C. Burla, M. Cavalli, G. Cascarano, C. Giacovazzo, A. Guagliardi, G. Polidori, R. Spagna, J. Appl. Crystallogr. 32 (1999) 115.

[39] S. Parkin, B. Moezzi, H. Hope, J. Appl. Crystallogr. 28 (1995) 53.